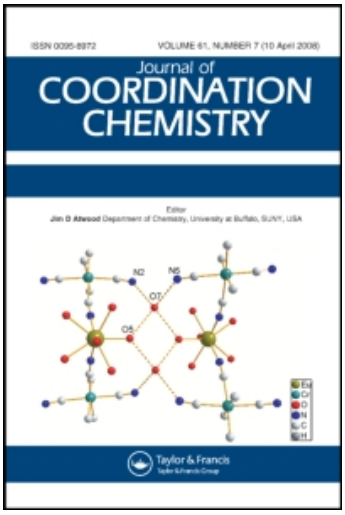

Journal of Coordination Chemistry
Publication details, including instructions for authors and subscription information:
http://www.informaworld.com/smpp/title~content=t713455674

Synthesis and metal(II) ion complexation of pyridine-2,6-diamides incorporating amino alcohols

Shi-Xia Luo[a]; Vanny Tiwow[b]; Marcel Maeder[b]; Geoffrey A. Lawrance[b]
[a] School of Physics and Chemistry, Guizhou Normal University, Guiyang 550001, P.R. China [b] Division of Chemistry, School of Environmental and Life Sciences, The University of Newcastle, Callaghan, N.S.W. 2308, Australia

First published on: 20 May 2010

To cite this Article Luo, Shi-Xia , Tiwow, Vanny , Maeder, Marcel and Lawrance, Geoffrey A.(2010) 'Synthesis and metal(II) ion complexation of pyridine-2,6-diamides incorporating amino alcohols', Journal of Coordination Chemistry, 63: 14, 2400 — 2418, First published on: 20 May 2010 (iFirst)
To link to this Article: DOI: 10.1080/00958972.2010.487562
URL: http://dx.doi.org/10.1080/00958972.2010.487562

Journal of Coordination Chemistry
Vol. 63, Nos. 14–16, 20 July–20 August 2010, 2400–2418

Synthesis and metal(II) ion complexation of pyridine-2,6-diamides incorporating amino alcohols§

SHI-XIA LUO†, VANNY TIWOW‡, MARCEL MAEDER‡ and GEOFFREY A. LAWRANCE*‡

†School of Physics and Chemistry, Guizhou Normal University, Guiyang 550001, P.R. China
‡Division of Chemistry, School of Environmental and Life Sciences, The University of Newcastle, Callaghan, N.S.W. 2308, Australia

(*Received 28 January 2010; in final form 25 February 2010*)

Reaction of 2,6-bis(methoxycarbonyl)pyridine with two equivalents of a β-amino alcohol yields pyridine-2,6-diamides $C_6H_3N(CONH–CR_1R_2–CHR_3–OH)_2$ [(**1**) $R_1=R_2=R_3=H$; (**2**) $R_1=R_2=H$, $R_3=CH_3$; (**3**) $R_1=CH_3$, $R_2=R_3=H$; (**4**) $R_1=C_2H_5$, $R_2=R_3=H$; (**5**) $R_1=C_6H_5CH_2$, $R_2=R_3=H$; (**6**) $R_1=O_2NC_6H_4CH(OH)$, $R_2=R_3=H$; (**7**) $R_1=R_2=CH_3$, R_3=H] incorporating the amino alcohols, several of which are chiral, whereas the free diamide ligands show no capacity toward deprotonation up to pH > 12. In the presence of metal(II) ions they undergo concomitant deprotonation and complexation to form [M(L-2H)] compounds. Formation constants have been determined for Cu(II), Ni(II), and Zn(II) complexes of the suite of ligands. Determined values for the two observed steps of $\log\beta_{ML\text{-}2H}$ and $\log\beta_{ML\text{-}3H}$ (where additional alcohol or coordinated water deprotonation occurs) are approximately −10 and −20, respectively. As pK_a values of the diamide cannot be determined independently, absolute $\log K_{ML\text{-}2H}$ values for the di-deprotonated complexes cannot be definitively assigned, although estimates are made using predicted pK_a values for the diamide. The circular dichroism spectra of optically active complexes were determined and are discussed.

Keywords: Pyridine-2,6-diamide; β-Amino-alcohol; Metal(II) complexation; Formation constants; Circular dichroism spectroscopy

1. Introduction

The development of ligand systems that contain pyridine-2-carboxamido functionality within larger ligand frameworks has been studied widely in recent years [1–9]. Molecules that contain the –HN–OC–pyridine–CO–NH– core have found wide application, with uses as diverse as components of electroluminescent devices to

*Corresponding author. Email: Geoffrey.Lawrance@newcastle.edu.au
§Dedicated to Prof Rudi van Eldik on the occasion of his 65th birthday in recognition of his contribution to coordination chemistry.

Journal of Coordination Chemistry
ISSN 0095-8972 print/ISSN 1029-0389 online
DOI: 10.1080/00958972.2010.487562

functioning as oxidation catalysts [8]. Recently, ligand systems based on the 2,6-diamidopyridine core that support helicate complex formation have been developed [3, 6, 8], and they represent a novel extension of this chemistry. This type of structure, however, appears to arise only in systems where favorable π–π stacking interactions support oligomer self-assembly. Yet the forces supporting helicate formation are subtle, it seems, as helicity is disrupted by even inserting an additional methylene in the pendant arm chain of a successful system [8, 9].

It is of interest to extend the examples of ligand systems with the 2,6-diamidopyridine core that have different terminal groups on the arms that offer strong capacity for hydrogen bonding interactions. Recently, 2,6-diamidopyridines with terminal saturated amines were examined [10], but found to form only simple mononuclear complexes in solution and the solid state. While a wide range of diamide ligands have now been reported, there has been little study of compounds with arms terminating in alcohol groups, particularly those that are chiral. Since amino alcohols (alkanolamines) offer two separate functional groups capable of both coordination and strong hydrogen bonding interactions, they present themselves as adequate ligands in their own right, and this capacity may be extended by incorporation into larger polydentate ligand systems. The synthesis of a series of diamides (**1**–**7**) based on compounds with C-substitution on the simple 2-aminoethanol parent, and aspects of their coordination chemistry are reported herein. With optically pure β-amino alcohols employed to prepare **3**–**6**, the study of the circular dichroism (CD) spectroscopy of these complexes is included.

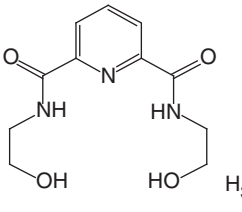

(1)

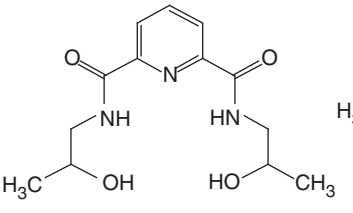

(2)

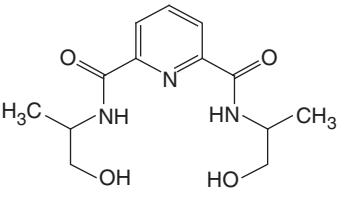

(3)

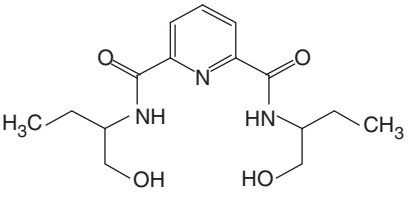

(4)

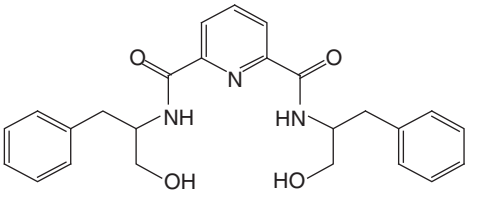

(5)

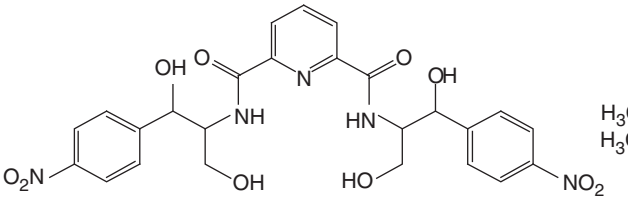

(6)

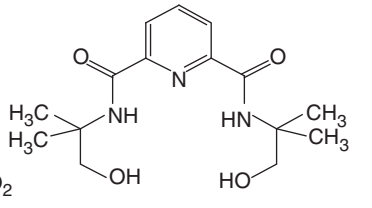

(7)

2. Experimental

2.1. *Ligand syntheses*

The precursor 2,6-pyridinedicarboxylic acid, 2,2-dimethoxypropane, and all β-amino alcohols were purchased (Aldrich) and used as received. Organic solvents were of analytical reagent (AR) grade and also used as received. Precursor 2,6-bis(methoxycarbonyl)pyridine was prepared analytically pure in almost stoichiometric yield (>95%), essentially as reported in [8], by refluxing (4 h) a mixture of 2,2-dimethoxypropane (80 mL), concentrated HCl (6.5 mL), and 2,6-pyridinedicarboxylic acid (10 g, 46 mmol) in methanol (200 mL), which formed white solid on cooling.

2.1.1. 2,6-Bis[N-(2′-hydroxyethyl)carbamoyl]pyridine (1). A solution of 2,6-bis (methoxycarbonyl)pyridine (0.97 g, 5 mmol) in toluene (30 mL) in a round-bottom flask was stirred and heated (60°C), and a solution of ethanolamine (0.79 g, 13 mmol) in toluene (11 mL) was added slowly from a dropping funnel. The mixture was heated and stirred (~100°C, 1 h) using an oil bath, then refluxed for 20 h; a pale yellow solid began to form after ~0.5 h. The heat was turned off and the mixture was allowed to cool slowly by stirring for further 24 h at room temperature. During this time, a further amount of solid precipitated; this was collected, washed in turn with diethyl ether (3 × 5 mL) and a small amount of chloroform, and air dried. Yield 1.17 g (92%). Anal. Calcd for $C_{11}H_{15}N_3O_4 \cdot \frac{1}{6}H_2O$ (%): C, 51.6; H, 6.0; and N, 16.4. Found (%): C, 51.9; H, 5.8; and N, 16.3. Nuclear magnetic resonance (NMR): $\delta_H(D_2O)$ 3.59 (4H, t, –CH_2–), 3.79 (4H, t, –CH_2–), and 8.15 (3H, m, pyH); $\delta_C(D_2O)$ 41.2 (–CH_2N), 59.6 (–CH_2O), 124.5, 139.4 (pyCH), 147.6 (pyC_{tert}), and 165.6 (C=O) ppm. IR: 3300 (OH), 2978, 2885, 1443, 1311, 1250, 1227 (CH), 1659 (CO), 1551 (NHCO), 1103, 1080, 1041, 1003, 849, 741, and 679 (py) cm^{-1}.

2.1.2. 2,6-Bis[N-(2′-hydroxypropyl)carbamoyl]pyridine (2). 2,6-Bis(methoxycarbonyl) pyridine (3.12 g, 16 mmol) in toluene (90 mL) was stirred and heated (60°C), and a solution of R-(+)-1-amino-2-propanol (2.85 g, 38 mmol) in toluene (30 mL) was added slowly. The mixture was heated and stirred (~95°C, 1 h), then refluxed for 24 h; a white solid began to form after ~10 h. The heat was turned off and the mixture was allowed to cool slowly while stirring for further 24 h at room temperature, after which a solid precipitate was collected as described for **1**. Yield 4.20 g (93%). Anal. Calcd for $C_{13}H_{19}N_3O_4 \cdot \frac{1}{6}H_2O$ (%): C, 54.9; H, 6.85; and N, 14.8. Found (%): C, 54.9; H, 6.9; and N, 14.8. NMR: $\delta_H(D_2O)$ 1.16 (6H, d, CH_3), 3.38 (4H, m, CH_2), 3.99 (2H, m, CH), and 8.08 (3H, m, pyH); $\delta_C(D_2O)$ 19.1 (CH_3), 45.9 (CH_2), 66.0 (CH), 124.5, 139.3 (pyCH), 147.5 (pyC_{tert}), and 165.3 (C=O) ppm. IR: 3325 (OH), 2970, 2932, 1450, 1304, 1242 (CH), 1682, 1666 (CO), 1543 (NHCO), 1126, 1088, 1003, 933, 849, 748, and 671 (py) cm^{-1}.

2.1.3. 2,6-Bis[N-(1′-methyl-2′-hydroxyethyl)carbamoyl]pyridine (3). 2,6-Bis(methoxycarbonyl)pyridine (0.98 g, 5 mmol) in toluene (30 mL) was stirred and heated (60°C), and a solution of R-(−)-2-amino-1-propanol (0.98 g, 13 mmol) in toluene (11 mL) was added slowly. The mixture was heated and stirred (~100°C, 1 h), and then refluxed for 24 h; a white solid was formed after ~5 h. Following further stirring for 24 h at room

temperature, a solid was collected as described for **1**. Yield 1.06 g (75%). Anal. Calcd for $C_{13}H_{19}N_3O_4 \cdot \frac{1}{3}H_2O$ (%): C, 54.35; H, 6.9; and N, 14.6. Found (%): C, 54.6; H, 6.9; and N, 14.6. NMR: $\delta_H(D_2O)$ 1.21 (6H, d, $-CH_3$), 3.67 (4H, m, CH_2), 4.20 (2H, m, –CH–), and 8.15 (3H, m, pyH). $\delta_C(D_2O)$ 15.3 ($-CH_3$), 47.1 (–CH–), 64.0 ($-CH_2-$), 124.7, 139.3 (pyCH), 148.0 (pyC_{tert}), and 165.9 (C=O) ppm. IR: 3400 (OH), 2970, 2885, 1450, 1365, 1250 (CH), 1682, 1643 (CO), 1543, 1512 (NHCO), 1149, 1095, 1034, 1003, 841, 748, and 679 (py) cm^{-1}.

2.1.4. 2,6-Bis[N-(1′-hydroxymethylpropyl)carbamoyl]pyridine (4). 2,6-Bis(methoxycarbonyl)pyridine (0.975 g, 5 mmol) in toluene (30 mL) was stirred and heated (60°C), and a solution of R-(−)-2-amino-1-butanol (1.16 g, 13 mmol) in toluene (11 mL) was added slowly. The mixture was heated and stirred (~105°C, 1 h), and then refluxed for 24 h, with a white solid forming after ~12 h. The heat was turned off and stirring was continued for 24 h. Then, the formed precipitate was collected as described for **1**. Yield 0.87 g (57%). Anal. Calcd for $C_{15}H_{23}N_3O_4 \cdot \frac{1}{4}H_2O$ (%): C, 57.4; H, 7.5; and N, 13.4. Found (%): C, 57.5; H, 7.3; and N, 13.3. NMR: $\delta_H(D_2O)$ 0.99 (6H, t, $-CH_3$), 1.72 (4H, m, $-CH_2-$), 3.81 (4H, m, $-CH_2-$), 4.13 (2H, m, –CH–), and 8.25 (3H, m, pyH). $\delta_C(D_2O)$ 9.4 ($-CH_3$), 23.1 ($-CH_2-$), 53.2 (–CH–), 63.0 ($-CH_2OH$), 124.8, 139.5 (pyCH), 148.2 (pyC_{tert}), and 166.0 (C=O) ppm. IR: 3395 (OH), 2962, 2878, 1427, 1358, 1250 (CH), 1682, 1643 (CO), 1543, 1520 (NHCO), 1126, 1088, 1057, 1003, 964, 818, 741, and 679 (py) cm^{-1}.

2.1.5. 2,6-Bis{N[(1′-hydroxymethyl-2′-phenyl)ethyl]carbamoyl}pyridine (5). To 2,6-bis (methoxycarbonyl)pyridine (0.10 g, 0.5 mmol) in a 25 mL flask, S-(−)-2-amino-3-phenyl-1-propanol (0.15 g, 1 mmol) was added. A microcondenser was fitted and the mixture was heated in a microwave synthesizer for 25 min on medium power. The resultant yellow oil was left to cool, and then diethyl ether (10 mL) was added. After an overnight stand, a pale yellow solid was collected and washed with a little water. The solid was then collected by vacuum filtration and air dried. Yield 0.088 g (40%). Anal. Calcd for $C_{25}H_{27}N_3O_4 \cdot \frac{1}{2}H_2O$ (%): C, 67.85; H, 6.4; and N, 9.5. Found (%): C, 67.5; H, 6.1; and N, 9.3. NMR: $\delta_H(CDCl_3)$ 2.98 (4H, m, $-CH_2-$), 3.46 (4H, m, $-CH_2-$), 3.74 (2H, m, –CH–), 4.31 (2H, s, –OH), 7.18 (10H, m, pyH), 7.90 (1H, t, pyH), 8.10 (2H, d, −NH–), and 8.22 (2H, d, pyH); $\delta_C(CDCl_3)$ 36.4 ($-CH_2-$), 52.5 (–CH–), 62.9 ($-CH_2OH$), 124.4 (pyCH), 126.1, 127.9, 128.8 (pyCH), 137.1 (pyCH), 138.4 (pyC_{tert}), 148.0 (pyC_{tert}), and 163.2 (C=O) ppm. IR: 3380 (OH), 2932, 2877, 1450, 1311, 1250 (CH), 1651 (CO), 1527 (NHCO), 1173, 1080, 1041, 1003, 841, 748, 702, and 648 (py) cm^{-1}.

2.1.6. 2,6-Bis{N[(1′-hydroxymethyl-2′-hydroxy-2′-(4″-nitrophenyl)ethyl]carbamoyl}pyridine (6). 2,6-Bis(methoxycarbonyl)pyridine (0.293 g, 1.5 mmol) and 1*S*,2*S*-(+)-2-amino-1-(4-nitro-phenyl)-1,3-propanediol (0.64 g, 3 mmol) were mixed in a flask which was then fitted with a microcondenser. The mixture was heated in a microwave synthesizer for 30 min on low power, and it resulted in a brown oily product. After an overnight stand at room temperature, diethyl ether (10 mL) was added. Further standing for 20 h resulted in a brown sticky solid, which was washed with water, diethyl ether, and chloroform. Drying yielded a light brown hygroscopic solid.

Yield 0.44 g (53%). Anal. Calcd for $C_{25}H_{25}N_5O_{10} \cdot \frac{1}{7}H_2O$ (%): C, 53.8; H, 4.6; and N, 12.5. Found (%): C, 54.1; H, 4.7; and N, 12.4. NMR: $\delta_H(CD_3COCD_3)$ 3.90 (4H, m, $-CH_2-$), 4.33 (4H, s, –OH), 5.31 (2H, m, –CH–), 5.50 (2H, m, –CH–), 7.74 (4H, d, pyH), 7.91 (2H, d, –NH–), 8.17 (4H, d, pyH), and 8.31 (3H, m, pyH). $\delta_C(CD_3COCD_3)$ 56.4 (–CH–), 61.1 ($-CH_2OH$), 69.9 (–CH–), 122.7, 124.3, 126.7, 138.5 (pyCH), 146.5, 148.3, 150.5 (pyC_{tert}), and 162.4 (C=O) ppm. IR: 3380 (OH), 2955, 2885, 1450, 1249 (CH), 1666 (CO), 1552, 1350 (NO_2), 1519 (NHCO), 1173, 1080, 995, 856, 748, and 684 (py) cm^{-1}.

2.1.7. 2,6-Bis[N-(1′,1′-dimethyl-2′-hydroxy)carbamoyl]pyridine (7). 2,6-Bis(methoxycarbonyl)pyridine (1.95 g, 10 mmol) in toluene (15 mL) was stirred and heated (85 C), and 2-amino-2-methyl-1-propanol (1.88 g, 21 mmol) was added slowly. The mixture was heated and stirred (~100°C, 0.5 h), and then refluxed for 48 h. The heat source was turned off, and the mixture was stirred for further 20 h. The white solid formed during this time was collected, washed under suction in turn with a little water and diethyl ether (3×5 mL), then finally air dried. Yield 2.47 g (80%). Anal. Calcd for $C_{15}H_{23}N_3O_4 \cdot \frac{1}{7}H_2O$ (%): C, 57.8; H, 7.5; and N, 13.4. Found (%): C, 57.8; H, 7.1; and N, 13.0. NMR: $\delta_H(CDCl_3)$ 1.49 (12H, s, $-CH_3$), 3.72 (4H, s, $-CH_2-$), 4.38 (2H, s, −OH), 8.05 (1H, t, pyH), 8.13 (2H, s, –NH–), and 8.31 (2H, d, pyH); $\delta_C(CDCl_3)$ 23.4 ($-CH_3$), 54.8 (−C–), 69.9 ($-CH_2-$), 123.9, 138.81 (pyCH), 148.1 (pyC_{tert}), and 162.6 (C=O) ppm. IR: 3395 (OH), 2970, 2939, 2870, 1458, 1365, 1281, 1219 (CH), 1682, 1659 (CO), 1520 (NHCO), 1165, 1065, 1018, 995, 903, 849, 756, and 679 (py) cm^{-1}.

2.2. *Syntheses of metal complexes*

Complexes were generally prepared by the reaction of diamide ligand and two equivalents of base with a metal(II) perchlorate salt; an alternative approach employed a metal acetate salt without the addition of base, relying on the basicity of this metal salt [8]. With the first method, solids which were isolated co-crystallized with various amounts of sodium perchlorate and/or water in their structures; perchlorate ion was evident in infrared (IR) spectra. Unfortunately, isolated crystals did not produce useful data sets for X-ray structure analysis. Isolated nickel(II) complexes were yellow-brown in color, a characteristic of square-planar diamagnetic species, also supported by the NMR spectra displayed. Copper(II) complexes isolated were blue-purple species consistent with their being traditional highly axially Jahn–Teller distorted octahedral (or pseudo square planar) monomers.

A general approach to synthesis using metal perchlorate salts was as follows. To a solution of diamide ligand (1.5 mmol) and NaOH (3 mmol) in methanol (~20 mL), a solution of metal(II) perchlorate (1.5 mmol) in methanol (~5 mL) was added slowly, followed by slowly adjusting the pseudo-pH to ~10 with NaOH in methanol solution. The resulting colored solution was stirred for ~0.5 h (Cu) or heated for 2 h at ~60°C (Ni), and then filtered to remove the traces of metal hydroxide solid. The filtrate was either used as collected (for Cu) or rotary evaporated to dryness and washed (diethyl ether, 2×20 mL), and then re-dissolved in a small volume (~10 mL) of methanol (for Ni). Upon standing in a sealed diethyl ether atmosphere, colored crystals formed after several days and were collected. The characterization for the complexes follows.

2.2.1. (2,6-Bis[N-(2′-hydroxyethyl)carbamido]pyridine)nickel(II), [Ni(1-2H)]. Yield 59%. Anal. Calcd for $C_{11}H_{13}N_3O_4Ni \cdot \frac{1}{2}H_2O \cdot \frac{1}{2}NaClO_4$ (%): C, 34.7; H, 3.7; and N, 11.05. Found (%): C, 34.5; H, 4.1; and N, 11.0. NMR: $\delta_H(D_2O)$ 3.60 (4H, t, $-CH_2-$), 3.83 (4H, t, $-CH_2-$), and 8.09 (3H, m, pyH). $\delta_C(D_2O)$ 40.9 ($-CH_2N-$), 59.4 ($-CH_2OH$), 124.2, 139.0 (pyCH), 147.0 (pyC_{tert}), and 165.0 (C=O) ppm. UV-Vis (water): λ_{max} 360 nm (ε_{max} 1790 $dm^3\,mol^{-1}\,cm^{-1}$), 435(sh). IR: 3480 (OH), 2947, 2885, 1450, 1419, 1358, 1311, 1250 (CH), 1651 (CO), 1551 (NCO), 1142, 1111, 1088, 934, 841, 733, 679 (py), 1100, and 620 (ClO_4^-) cm^{-1}.

2.2.2. (2,6-Bis[N-(2′-hydroxypropyl)carbamido]pyridine)nickel(II), [Ni(2-2H)]. Yield 44%. Anal. Calcd for $C_{13}H_{17}N_3O_4Ni \cdot H_2O$ (%): C, 43.9; H, 5.4; and N, 11.8. Found (%): C, 44.2; H, 5.4; and N, 11.5. NMR: $\delta_H(D_2O)$ 1.26 (6H, d, $-CH_3$), 3.49 (4H, m, $-CH_2-$), 4.12 (2H, m, –CH–), and 8.19 (3H, m, pyH); $\delta_C(D_2O)$ 19.5 ($-CH_3$), 46.3 ($-CH_2-$), 66.5 (–CH–), 125.0, 139.8 (pyCH), 147.9 (pyC_{tert}), and 165.9 (C=O) ppm. UV-Vis (water): λ_{max} 340 nm (ε_{max} 1448 $mol^{-1}\,cm^{-1}$), 435(sh). IR: 3425 (OH), 2978, 2932, 1450, 1327 (CH), 1682, 1651 (CO), 1543 (NCO), 1142, 1119, 1088, 1003, 926, 841, 733, and 679 (py) cm^{-1}.

2.2.3. (2,6-Bis[N-(1′-methyl-2′-hydroxyethyl)carbamido]pyridine)nickel(II), [Ni(3-2H)]. Yield 23%. Anal. Calcd for $C_{13}H_{17}N_3O_4Ni \cdot 1\frac{1}{2}NaClO_4 \cdot \frac{1}{2}H_2O$ (%): C, 29.4; H, 3.5; and N, 7.9. Found (%): C, 29.3; H, 3.8; and N, 7.5. NMR: $\delta_H(D_2O)$ 1.31 (6H, d, $-CH_3$), 3.76 (4H, m, $-CH_2-$), 4.31 (2H, m, –CH–), and 8.21 (3H, m, pyH); $\delta_C(D_2O)$ 15.2 ($-CH_3$), 47.0 (–CH–), 63.9 ($-CH_2-$), 124.6, 139.1 (pyCH), 147.8 (pyC_{tert}), and 165.1 (C=O) ppm. UV-Vis (water): λ_{max} 363 nm (ε_{max} 1995 $mol^{-1}\,cm^{-1}$), 435(sh). IR: 3550, 3402 (OH), 2970, 2885, 1450, 1249 (CH), 1682, 1643 (CO), 1589, 1543, 1520 (NCO), 1142, 1088, 1034, 1003, 841, 748, 679 (py), 1100, and 618 (ClO_4^-) cm^{-1}.

2.2.4. (2,6-Bis[N-(2′-hydroxyethyl)carbamido]pyridine)copper(II), [Cu(1-2H)]. Yield 71%. Anal. Calcd for $C_{11}H_{13}N_3O_4Cu \cdot \frac{1}{2}NaClO_4 \cdot 1\frac{1}{2}H_2O$ (%): C, 32.7; H, 4.0; and N, 10.4. Found (%): C, 32.6; H, 3.85; and N, 10.2. UV-Vis (water): λ_{max} 615 nm (ε_{max} 154 $mol^{-1}\,cm^{-1}$). IR: 3455 (OH), 2962, 2862, 1427, 1381 (CH), 1651 (CO), 1574, 1528 (NCO), 1119, 1080, 1041, 941, 858, 756, 687 (py), 1105, and 624 (ClO_4^-) cm^{-1}.

2.2.5. (2,6-Bis[N-(2′-hydroxypropyl)carbamido]pyridine)copper(II), [Cu(2-2H)]. Yield 60%. Anal. Calcd for $C_{13}H_{17}N_3O_4Cu \cdot \frac{3}{4}NaClO_4 \cdot \frac{1}{2}H_2O$ (%): C, 35.9; H, 4.2; and N, 9.6. Found (%): C, 35.9; H, 4.5; and N, 9.45. UV-Vis (water): λ_{max} 603 nm (ε_{max} 163 $mol^{-1}\,cm^{-1}$). IR: 3385 (OH), 2970, 2908, 1427, 1381, 1304 (CH), 1651 (CO), 1574 (NCO), 1119, 1080, 1041, 926, 841, 756, 687 (py), 1095, and 619 (ClO_4^-) cm^{-1}.

2.2.6. 2,6-Bis[N-(1′-methyl-2′-hydroxyethyl)carbamido]pyridine, [Cu(3-2H)]. Yield 37%. Anal. Calcd for $C_{13}H_{17}N_3O_4Cu \cdot 1\frac{1}{2}NaClO_4 \cdot \frac{1}{2}H_2O$ (%): C, 29.2; H, 3.5; and N, 7.8. Found (%): C, 29.4; H, 3.8; and N, 7.4. UV-Vis (water): λ_{max} 581 nm (ε_{max} 152 $mol^{-1}\,cm^{-1}$). IR: 3400 (OH), 2939, 2885, 1450, 1249 (CH), 1682, 1643 (CO), 1589, 1542, 1512 (NCO), 1149, 1034, 1003, 864, 748, 679 (py), 1095, and 618 (ClO_4^-) cm^{-1}.

2.2.7. (2,6-Bis[N-(1′,1′-dimethyl-2′-hydroxy)carbamido]pyridine)copper(II), [Cu(7-2H)]. Yield 57%. Anal. Calcd for $C_{15}H_{21}N_3O_4Cu \cdot \frac{1}{4}NaClO_4 \cdot \frac{1}{2}H_2O$ (%): C, 43.9; H, 5.4; and N, 10.1. Found (%): C, 44.2; H, 5.45; and N, 9.7. UV-Vis (water): λ_{max} 627 nm (ε_{max} 148 $mol^{-1}\,cm^{-1}$). IR: 3365 (OH), 2962, 2932, 2816, 1450, 1373, 1304, 1250 (CH), 1666, 1635 (CO), 1605, 1581, 1535 (NCO), 1173, 1067, 1041, 987, 841, 764, 687 (py), 1100, and 622 (ClO_4^-) cm^{-1}.

2.3. *Physical methods*

NMR spectra were recorded on solutions of ligands and complexes in $CDCl_3$, D_2O or CD_3COCD_3 using a Bruker DPX300 spectrometer; Fourier transform infrared (FT-IR) spectra were recorded on a Shimadzu FT-IR-8400 spectrophotometer with KBr disks. UV-Vis spectroscopy in water or methanol solution employed a Hitachi U-2000 spectrophotometer. CD spectra were measured in methanol using an Applied Photophysics Chirascan spectrophotometer. For the CD spectroscopy, free ligands were made up to suitable concentrations in methanol, whereas for complexes 10^{-2} M M^{2+} (Cu^{2+}, Co^{2+}, Ni^{2+}, Zn^{2+}, Mn^{2+}) solutions in methanol were added to 10^{-2} M ligand solutions in methanol that also contained 2 equivalents of NaOH. Apart from M : L = 1 : 1, experiments with M : L = 3 : 2 or 2 : 3 showed no significant difference in the CD spectrum, consistent with the formation of dominantly 1 : 1 species in solution. Microanalyses were performed by the microanalytical unit of the Australian National University.

Equilibrium constants ($\log \beta$) for protonation equilibria and metal–ligand complexation were determined by employing data collected by a fully computerized potentiometric titration setup comprising a Metrohm combined glass electrode (6.0234.100) read by a PCI-6014 NI-DAQ data acquisition board and a Metrohm 665 Dosimat burette. All titrations were performed under a nitrogen atmosphere at 25 ± 0.1°C. The solution of the ligand (5×10^{-3} $mol\,dm^{-3}$) alone containing 3.5–5.5 equivalents of excess acid ($HClO_4$) and in the presence of 0.9 or 0.5 or 0.3 equivalents of metal ion were titrated with a 0.1 $mol\,dm^{-3}$ NaOH solution. An established in-house software was employed for data analysis.

3. Results and discussion

3.1. *Ligand synthesis and characterization*

The suite of symmetrically armed diamide compounds **1**–**7** were prepared using 2,6-bis(methoxycarbonyl)pyridine as the core reagent, which reacted with the primary amine group of a β-amino-alcohol. Conventional reflux in an organic solvent was usually successful; however, solvent-free reaction in a microwave reactor was used for **5** and **6**, where bulky aromatic substituents are attached to the amino alcohol framework, in order to drive the reaction to completion. These two latter syntheses did not proceed cleanly by refluxing in toluene, with a mixture of the one-armed monoamide and the diamide formed, from spectroscopy. Possibly, conventional reaction with an acid chloride rather than an ester may have been more successful,

Table 1. NMR chemical shifts (ppm) for the 2,6-bis(methoxy-carbonyl)pyridine precursor and **1** and **2**.

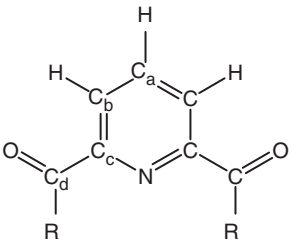

Precursor **1** **2**

R = 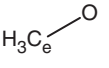

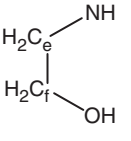

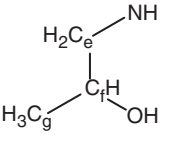

Assignment	Category	Precursor	**1**	**2**
C_a	pyC_H	138.3	139.4	139.3
C_b	pyC_H	128.0	124.5	124.5
C_c	pyC_{tert}	148.0	147.6	147.5
C_d	>C=O	165.0	165.6	165.3
C_e	CH_3–O– or –CH_2–R–	53.2	41.2	45.9
C_f	–CH_2–OH or –CH(R)–OH	–	59.6	66.0
C_g	CH_3–C–	–	–	19.1
HC_a	pyH	8.30	8.15	8.08
HC_b	pyH	8.02	8.15	8.08
HC_e	CH_3–O– or –CH_2–R–	4.00	3.59	3.38
HC_f	–CH_2–O– or –CH(R)–O–	–	3.79	3.99
HC_g	CH_3–C–	–	–	1.16

but the microwave method supplied the answer to low reactivity without the need to change the key reagent.

Compounds isolated were microanalytically pure, but were also readily characterized spectroscopically, with ^{13}C- and ^{1}H-NMR particularly revealing the constituents. The parent 2,6-bis(methoxycarbonyl)pyridine has five distinct carbons as a result of symmetry, whereas in the ^{1}H-decoupled ^{13}C-NMR the three aromatic resonances are assigned to C_a (138.3), C_b (128.0), and the tertiary C_c (148.0), with the amide resonance (C_d) at 165.0 and the ester methyl group resonance (C_e) at 53.2 ppm (refer to table 1 for carbon identification). The ^{1}H-NMR is simple; the uncoupled methyl (H_3C_e) of the ester appears as a singlet at 4.0 ppm, whereas the two types of aromatic protons on the pyridine form the expected and distinctive doublet and triplet (at 8.0 (for HC_b) and 8.3 (for HC_a) ppm, respectively) in a 2 : 1 ratio. Introduction of the aminoethanol arms in place of the ester groups means that at least two more new carbon centers are introduced, whereas the ester methyl group is lost; for the parent 2-aminoethanol

leading to **1**, this is the case, whereas other C-substituted aminols lead to a more complex spectra, such as in **2**. For **1**, the methylenes introduced with the aminol have distinctively different ^{13}C chemical shifts due to the different adjacent heteroatoms, 41.2 (C_e–N) and 59.6 (C_f–O) ppm. Other carbons have chemical shifts like those in their 2,6-bis(methoxycarbonyl)pyridine parent (table 1). With **2**, the ^{13}C chemical shifts are overall similar to those in **1**, although an additional signal characteristic of the extra methyl group is present at 19.1 ppm. Other analogs can likewise be assigned effectively (detailed in section 2).

IR spectra provide additional support for the structures. The parent diester has a strong and characteristic ester resonance at 1740 cm^{-1} and other carbonyl resonances at 1290 and 1243 cm^{-1}. A range of resonances associated with the pyridine ring occur: inplane C=C resonances at 1572, 1453, and 1434 cm^{-1}; pyridine breathing modes at 1165, 1145, and 996 cm^{-1}; bands from out-of-plane resonances characteristic of 2,6-disubstituted pyridines at 949, 852, 813, and 756 cm^{-1}. Similar resonances occur in all the ligands prepared. In IR spectra of the amides, the ester resonance in the parent molecule is absent, and strong resonances associated with the amide (1520–1580, 1420–1460 cm^{-1}) and carbonyl groups (1640–1680 cm^{-1}) replace it. The methylenes in **1** and its analogs give rise to strong resonances in the IR spectra between 2860 and 2980 cm^{-1}. The most characteristic pyridine resonances are those at ~740 and ~680 cm^{-1}. The presence of the alcohol is associated with a fairly sharp stretching vibration near 3300 cm^{-1}.

Pyridine-2,6-diamide molecules are now well known and well characterized. There have been several examples characterized by X-ray crystal structure analyses; one recent example involves a diamide terminated by saturated amine pendant arms [10]. The spectroscopy of this firmly defined amido-amine species is very similar to that observed here for the amido-alcohol series, supporting the structural assignments made here for this new family of analogs based on amino-alcohol precursors. The structures assigned to the new ligands developed here appear sound, from spectroscopic characterization and comparisons with known close analogs.

3.2. *Formation of complexes*

3.2.1. Syntheses. Complexation of the diamide ligands occurs with the deprotonation of the amide groups, so that the complexes formed include diamido dianionic ligands and are neutral for metal(II) species. The amido group is a significantly better donor than the protonated amide form, and few examples of coordinated and protonated amides have appeared. Apart from the obvious change in the charge of the complex upon ligand binding, one of the simplest identifiers is the loss of the strong amide band at ~1670 cm^{-1} in the IR spectrum, to be replaced by bands from the amido group (~1560 cm^{-1}). The free amide ligands do not undergo deprotonation until beyond a pH of 12; complexation changes the amide acidity significantly. Further, the alcohol group also is more acidic when coordinated, with the anion a better donor than the neutral alcohol; however, deprotonation associated with this coordinated group occurs at a higher pH than for amides. Examples of neutral diamido complexes of Ni(II) and

Cu(II) were prepared and isolated successfully in this study, and all of them display apparently 1 : 1 M : L binding.

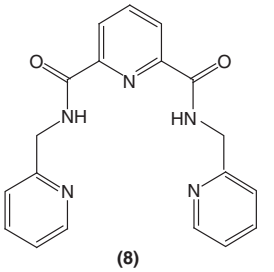

(8)

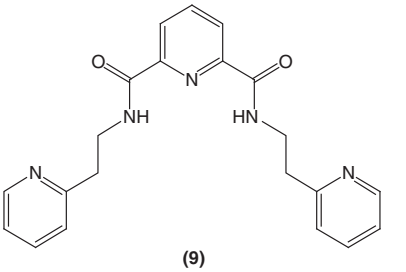

(9)

Earlier, the complexation of 2,6-bis[*N*-(2′-pyridyl-methyl)carbamoyl]pyridine, **8**, was reported [8], with this diamide ligand showing a strong tendency to form helical species on complexation. Helical structures have been characterized by X-ray crystal structures in dinuclear M_2L_2, trinuclear M_3L_2 and tetranuclear $M_4L_2L'_2$ complexes of **8**; further, some simple mononuclear ML complexes have been defined [8]. The close analog involving pendant pyridine connection to an amide by two methylene groups, **9**, rather than the one methylene group in **8**, however, shows no tendency toward helicate formation [9], suggesting that the forces that control helicate formation are subtle and such behavior may not commonly occur. Similar ligands terminating with saturated amine groups in the place of pyridine show no evidence of helicate formation with metal(II) ions; in solution, electrospray ionization–mass spectrometry (ESI–MS) shows no peaks assignable to polynuclear species [10]. Complexation of a range of other pyridine diamide ligands has been examined. For example, the copper(II) complex of **10** reportedly binds copper(II) as a 1 : 1 M : L species to form a pentadentate mononuclear copper(II), one among a number of mononuclear copper(II) complexes that contain dicarboxamido ligation in CuN_5 chromophores [11].

Given the apparent inability of diamides with flexible pendant chains terminating with saturated primary amines to participate in complexations other than simple 1 : 1, a similar behavior observed here with diamides carrying flexible pendant chains terminating in alcohol groups is not unexpected. This is despite both amine and alcohol terminal groups being capable of participating in strong hydrogen bonding interactions. Complexation of **2**–**7** has also been explored, apart from the isolation of some selected complexes, through potentiometric titrations in solution, described later.

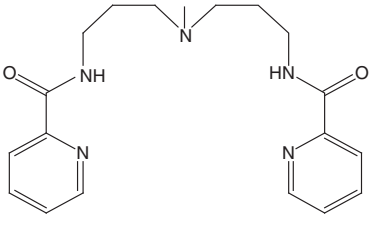

(10)

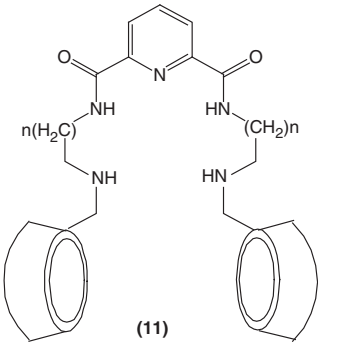

(11)

Ligands developed herein present a N_3O_2 donor set, but their spectroscopic behavior in solution is consistent with a dominantly monomeric pseudo square-planar MN_3O core, although weak axial binding of the remaining pendant alcohol may occur. Cu(II) forms complexes with electronic absorption maxima near 600 nm, which is appropriate for CuN_3O coordination in a plane around the metal ion. The Ni(II) complexes isolated are diamagnetic and have electronic absorption maxima below 400 nm, appropriate for low-spin square-planar Ni(II); presumably, the three aromatic nitrogen donors provide a sufficiently strong ligand field to enforce this outcome.

Overall, it appears that 2,6-diamidopyridines with two identical pendant chains including at least two methylene groups show no tendency toward helicate formation irrespective of the type of donor group terminating the chains. For aliphatic-terminated ligands, the loss of ability of the pendants to participate in π-stacking, found to stabilize helicates with **8**, further restricts the likelihood of helicate formation. Here, even the addition of an aromatic ring on the pendant chain in **5** and **6** does not lead to helicates. It is notable that polynuclear helicates of this class of ligand have high aromaticity, and the failure of the more saturated ligand systems examined here and elsewhere [10] to helicate indirectly supports a role for aromatic groups as structure makers. Systems with non-equivalent arms, including aromatic and aliphatic ones, have been addressed recently; these do not readily form helicates, but there is some limited evidence that they can exist [12]. Nevertheless, among a wide variety of diamide ligand systems now reported, few, irrespective of the type of pendant groups involved, showed a tendency toward helicate formation. This supports the view that stabilization of helicates is not routinely promoted simply by the presence of the –NHCO–py–CONH– core, and that the character of the pendant groups is particularly important; otherwise, conventional coordination chemistry results. A more extensive examination of the coordination of these new ligand systems to inert metal ions could be of some interest, although complexation has been defined adequately here.

3.2.2. Potentiometric titrations. Potentiometric titration of the free ligands up to a pH of ~13 exhibited no steps that could be assigned to deprotonation phenomena, consistent with the known behavior of amides, which have pK_a values such that free amides cannot be deprotonated in aqueous solution. However, for titration of amides **1**–**7** with one equivalent of Cu(II), Ni(II) or Zn(II) also present, a common form of speciation curve consistent with two deprotonation and complexation phenomena was observed, as exemplified in figure 1. For these curves, a common model could be employed, fitting ML-2H and ML-3H species only, both clearly distributed. In most cases, the fit was exceptionally good; where there were some problems with fitting, these arose from precipitation and for a limited number of cases this occurred too early in the titration to allow successful fitting. However, in most cases, successful log β values were determined, and are given in table 2. The presence of a ML-2H species in solution is fully consistent with the crystallization of neutral species of this formulation as solids from solution. From spectroscopic and structural evidence, they correspond to diamido species, where the two amide groups are both deprotonated and coordinated. The second step leading to a ML-3H species involves deprotonation of either a coordinated water or alcohol, which is discussed in detail later.

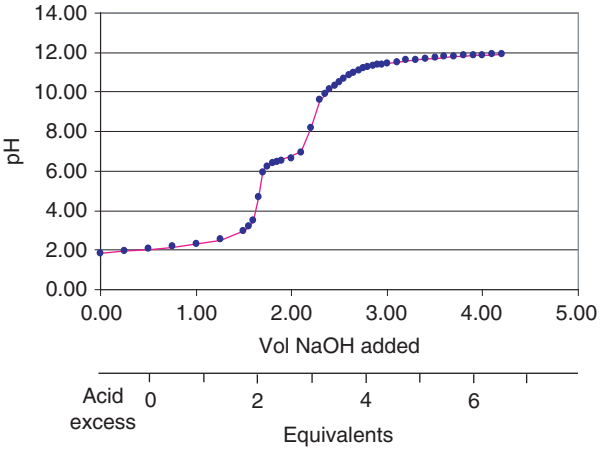

Figure 1. An example of the potentiometric titration curve (✱✱✱) overlayed with the calculated fit (——) for **2** in the presence of a molar equivalent of Cu(II).
Notes: In the absence of the metal ion, no steps are observed below a pH of 12. (Both volume and molar equivalents of the base added are represented on the axis; initial addition of a calculated amount of excess acid means the zero point for equivalents is displaced.)

Table 2. Formation constants (log β) for complexation of pyridine diamide-dialcohol ligands **1**–**7** with several metal(II) ions.

Ligand	Formed species	Cu(II)	Ni(II)	Zn(II)
1	ML-2H	-10.33 ± 0.03	-13.90 ± 0.03	-11.44 ± 0.06
	ML-3H	-20.18 ± 0.04	-26.48 ± 0.03	-21.42 ± 0.13
2	ML-2H	-10.47 ± 0.02	Precipitation	-11.41 ± 0.05
	ML-3H	-20.32 ± 0.04		-22.87 ± 0.20
3	ML-2H	-10.42 ± 0.02	-14.32 ± 0.05	-11.44 ± 0.04
	ML-3H	-20.47 ± 0.04	-22.63 ± 0.06	-21.04 ± 0.08
4	ML-2H	-10.65 ± 0.02	-13.88 ± 0.08	-11.19 ± 0.14
	ML-3H	-21.54 ± 0.06	-26.7 ± 0.8	-21.16 ± 0.25
5	ML-2H	-11.61 ± 0.01	-12.37 ± 0.17	–
	ML-3H	-21.76 ± 0.01	-22.3 ± 0.5	–
6	ML-2H	-10.2 ± 0.2	-13.2 ± 0.5	–
	ML-3H	-19.8 ± 0.3	-21.7 ± 0.5	–
7	ML-2H	-10.29 ± 0.04	Precipitation	Precipitation
	ML-3H	-20.78 ± 0.06		

The process of complexation in this case is a composite one involving two deprotonations along with coordination of the metal to the two amido groups, i.e.,

$$M^{2+} + L - 2H^{+} = [M(L^{2-})] \quad (1)$$

and occurs around a pH of ~5. Previously, pyridine diamides of the family **11** with appended cyclodextrins were prepared [13] and complexation with Cu(II) examined, where diamide deprotonation promoted by Cu(II) occurs at a pH of ~6. The similarity is notable. These pyridine diamide ligands show greater apparent acidity than peptides

or analogous amides undergoing complexation and deprotonation, where pK_a values in the range 9–12 have been reported [14–17]; this relates to the significantly different groups with different electronic effects attached to the amides.

The log β values associated with ML-2H formation for the suite of ligands **1**–**7** are very similar for any particular metal ion, consistent with their common ligand framework, with differences associated with the steric and electronic effects of substituents on carbon atoms of the amino alcohol residue chains. However, differences between metal ions are observed, with log β varying from approximately −10.5 for Cu(II) to −14 for Ni(II) and to −11.5 with Zn(II). This variation reflects both the differing effect of the metal ion on the amide pK_a and the different strengths of complexation by the metal ions. It is difficult to separate out the various individual components. The overall equation for this step (equation (1)) may be written as a series of sequential steps (equations (2)–(4)):

$$L - H^+ = L^- \quad (K_1) \tag{2}$$

$$L^- - H^+ = L^{2-} \quad (K_2) \tag{3}$$

$$M^{2+} + L^{2-} = [M(L^{2-})] \quad (K_3) \tag{4}$$

The three constants associated with these steps contribute to the overall composite β ($\beta = K_1 \cdot K_2 \cdot K_3$). Only if estimates can be made for independent K_1 and K_2 values can the formation constant for the complex be estimated. Since the pK_a of coordinated amines are typically in the range 9–12 and coordinated water and alcohols have values in the range 6–10, it seems likely that the pK_a of a coordinated amide group could be ~9 (and higher, possibly ~11, for the second deprotonation). Assigning these values to K_1 and K_2 leads to log $K_3 \approx 10$ for the Cu(II) complexes. Since we are dealing with a polydentate ligand with favored *N* and *O* donors, this is a reasonable value for the stability constant. However, in light of the fact that the deprotonation constants are not measurable separately, it would be of no value to speculate further. The overall log β values do suggest that, in general (and assuming amide pK_a values are closely similar with each metal(II) ion), the Ni(II) complexes are less stable than Cu(II), with Zn(II) also less stable than the latter. The apparently higher stability for Cu(II) is consistent with the usual expectations for first-row transition metal ions.

The second step in each titration is associated with a following single deprotonation. Such deprotonation processes for complexes at high pH are not unusual and are almost always associated with deprotonation of a coordinated ligand, often a coordinated water. The presence of alcohol groups provides the opportunity for a competing deprotonation to that from water. The diamido ligand will bind the metal ion with three *N*-donors from the pyridine and two amido groups required to lie in a plane with the metal ion. Additional donors are required to complete the coordination sphere in a 1 : 1 M : L complex, which will certainly be greater than three. Depending on the coordination number (4, 5 or 6), one, two or three additional groups may be attached. Acidity of the alcohol groups in the arms will be significantly enhanced on coordination, as for water. As this appears to be a simple single process, the pK_a value for this step can be determined from the difference in log β values in table 2 and it is of the order of 10 across the series of measurements, but varies slightly with metal ion

and ligand. A pK_a of ~10 is not inconsistent with the values expected for coordinated ROH groups on metal(II), and thus this assignment is supported by this observation.

3.3. *CD spectroscopy*

Of the amino alcohol precursors that produce **1**–**7**, only those used for **1** and **7** have no chiral carbon. The others were obtained commercially as one pure optical isomer except for **2**, leading to the synthesized molecules **3**–**6** also being chiral, since their syntheses did not involve any chemistry at the center of chirality that could lead to racemization. CD spectroscopy is particularly sensitive to coordination geometry and the mode of ligand binding [18], and also offers a potentially different method for measuring formation constants that will be explored elsewhere.

Whereas the parent amino alcohols offer at best bidentate chelation, the present set of ligands has up to five groups that may participate as donors. With the center of chirality lying in the alcohol pendant arms, CD spectroscopy may provide some indication of whether the alcohol groups are coordinated in solution, since the CD spectrum is anticipated to vary depending on whether or not the arms terminating with alcohol groups bind, adding chelate rings. Prospects are discussed below in the context of a distorted octahedral geometry. What should also be noted is that if the complex in solution adopts a five- or even four-coordinate geometry, this will alter the order and separation of the energy levels and also affect the CD pattern observed.

The central *N*,*N*′,*N* core of the ligand is presumed to bind efficiently to Cu(II) in solution, and this is observed in all solid state structures of related complexes. As a consequence, variation in coordination will depend on the binding of the pendant arms; some examples of species possible in solution are presented below (scheme 1) based on an octahedral core. The geometry in solution need not correspond to that in the solid state for complexes of labile metal ions.

In principle, there are three classes of complexes likely in solution, involving no pendant arms bound (a), one bound (b) or both bound (c); of course, there are other diastereomers possible, but these are not at the core of the following discussion and so are not presented. Conformational effects usually dominate vicinal effects, so the variation from two to three to four chelate rings in stepping from (a) to (b) to (c) suggests that the overall strength of the CD should increase in that order. The location of the chiral centers in all but **2** places this adjacent to the imido nitrogen, and thus it influences the rotatory strength effectively in all coordination modes. The incorporation

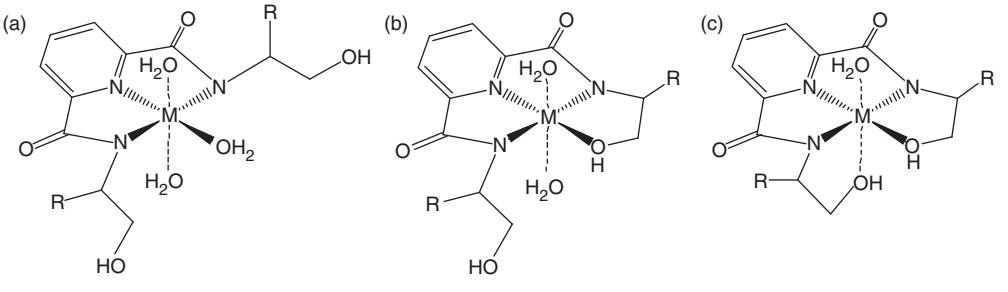

Scheme 1. Possible ligand binding modes.

of the chiral center in a chelate ring usually leads to a particularly significant enhancement [18], suggesting that the CD intensity should vary in the order (c) > (b) > (a). Of course, since the observed CD is the result of the summation of bands of different possible signs and bandwidths, the shifts in peak positions and bandwidth alone can lead to changes that may not reflect the actual changes in rotational strength [19]. So the outcomes of these comparisons need to be taken with some caution in any case.

The d^9 Cu(II) is found in a Jahn–Teller distorted environment, and as a consequence, the parent ^2E_g ground state and the $^2T_{2g}$ level split into $^2B_{1g}$, $^2A_{1g}$ and $^2B_{2g}$, ^2E_g levels, respectively, in the order of increasing energy. This leads to three spin-allowed transitions, $^2B_{1g} \rightarrow {}^2A_{1g}$ (although magnetic dipole forbidden), $^2B_{1g} \rightarrow {}^2B_{2g}$ and $^2B_{1g} \rightarrow {}^2E_g$. The energy separation between the three excited states are relatively small and under some circumstances, levels may even be nearly degenerated [20]. Further, the doubly degenerated ^2E_g level may be split into $^2\Gamma_a$ and $^2\Gamma_b$ components by spin-orbit coupling, meaning that there are effectively four closely-spaced bands under the $^2E_g \rightarrow {}^2T_{2g}$ cubic band envelope. This results in a broad indistinct absorption band in the visible spectrum, although in the CD spectrum a number of bands (some of opposite sign) may be observed, reflecting more effectively the complex nature of the Cu(II) electronic spectrum. The observed Cotton effect depends on the relative rotational strengths of the four components, and these will change as the chiral ligands and or mode of coordination change. The presence of asymmetric centers in the coordinated ligands (the vicinal effect) and ligand chelation forming a non-planar ring (the conformational effect, usually more significant [18]) may both contribute to the size of the CD signal. Prior studies suggest that as many as four CD bands of differing sign patterns can indeed be observed for Cu(II) complexes [20, 21].

A typical example of the visible and CD spectra for Cu(II) complexes of the chiral ligands **3**–**6** appears in figure 2, with all data given in table 3. The absorption spectra of

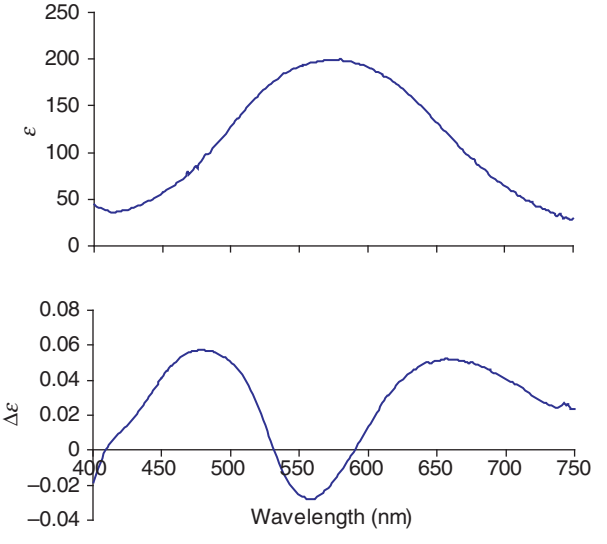

Figure 2. Visible absorbance (top) and CD (bottom) spectra of Cu^{II}(**3**-2H) measured in aqueous solution.

Table 3. Absorbance and CD spectral maxima for 1 : 1 M : L complexes of **1**–**7**.

L	M	UV-Vis spectrum λ_{max}, nm (ε_{max}, $(mol\,L^{-1})^{-1}\,cm^{-1}$)	CD spectrum λ_{max}, nm ($\Delta\varepsilon_{max}$, $(mol\,L^{-1})^{-1}\,cm^{-1}$)
1	None	196 (3510)	–[a]
	Cu(II)	586 (154)	–[a]
	Ni(II)	374 (3250), 435sh (900)	–[a]
	Zn(II)	266 (880)	–[a]
2	None	198 (6740)	–[b]
	Cu(II)	572 (164)	–[b]
	Ni(II)	376 (4510), 435sh (1100)	–[b]
	Zn(II)	266 (765)	–[b]
3	None	198 (5552)	196 (+8.28)
	Cu(II)	580 (200)	657 (+0.052), 560 (−0.028), 475 (+0.057)
	Ni(II)	375 (6450), 435sh (1700)	463 (+1.008), 369 (−0.663)
	Zn(II)	263 (574)	276 (−0.19)
4	None	200 (4820)	197 (+7.86)
	Cu(II)	579 (197)	644 (+0.051), 548 (−0.004), 476 (+0.057)
	Ni(II)	375 (3020), 440sh (820)	675 (+0.127), 455 (+0.239), 367 (−0.073)
	Zn(II)	261 (535)	265 (+0.21)
5	None	268 (4955)	244 (−35.0)
	Cu(II)	585 (186)	745 (−0.070), 515 (−0.428)
	Ni(II)	378 (3760), 445sh (950)	502 (+0.268), 431 (−1.000), 367 (+0.270)
	Zn(II)	270 (745)	281(−1.52)
6	None	271 (6200)	285 (+3.06), 260 (−0.38)
	Cu(II)	596 (101)	725sh (+0.078), 562 (+0.220), 440 (−0.002)
	Ni(II)	379 (5650), 440 (770)	483 (+1.178), 420sh (+0.678), 368 (−1.668)
	Zn(II)	272 (1100)	292 (+0.39), 255 (−0.040)
7	None	200 (2460)	–[a]
	Cu(II)	600 (149)	–[a]
	Ni(II)	376 (6110), 445sh (1300)	–[a]
	Zn(II)	268 (1070)	–[a]

[a]Achiral ligand; no CD possible.
[b]Only the racemic ligand available; no CD recordable.

the Cu(II) complexes all have maxima in a narrow range around 590 nm, consistent with coordination of three nitrogen donors to copper; in general, the maximum shifts to longer wavelength as the number of *N*-donors is reduced, with four *N*-donors typically leading to a maximum near ~550 nm, three *N*-donors ~600 nm and two *N*-donors ~650–700 nm. This suggests that, as anticipated, the central *N*,*N*′,*N* core of the ligand is bound to the metal ion in solution.

In the CD spectra, the average intensity of Cotton effects increases in the order **(6)** > **(5)** > **(4)** > **(3)**, which relates to the relative size of the R-group attached to the asymmetric carbon centers. Since rotational strengths from the vicinal and conformational effects are both influenced by substituent size [18], this is an anticipated result. The almost 10-fold increase in the size of the Cotton effects across the series is notable, but it is similar to the variation in intensity found for the vicinal effect in complexes of simple asymmetric unidentate amines [22], where the chiral center is the same number of bonds from a donor atom as in the present complexes.

The CD of simple chiral amino alcohol complexes of Cu(II) has been reported [23–26]. These form five-membered chelate rings that are conformationally similar to five-membered diamine chelate rings, but the chiroptical properties differ because different

chromophores are involved. Despite this, both systems exhibit strong Cotton effects as chelates associated with the strong conformation effect of the puckered rings. In addition, the amino alcohols show a marked pH dependence associated with the deprotonation of the alcohol. In this case, the N,N',N core chelating unit is essentially flat as a result of the aromatic ring, so its conformation effect will be diminished. Thus, the relatively large Cotton effects seen may indicate that at least one alcohol arm is bound (as in (b) in scheme 1), forming a puckered chelate ring and locating a chiral center closer to the metal.

The nickel(II) complexes display absorption spectra consistent with a formulation, supported by NMR spectroscopy, as diamagnetic low-spin d^8 systems. It is assumed that coordination is square planar, similar to that reported for analogous ligands [8]. While one alcohol group can bind as in (b) of scheme 1, the other must remain free since the coordination sphere is satisfied by binding the first group. There is no special pH dependence expected with a pendant alcohol group, as it can neither be protonated nor deprotonated in accessible pH regimes. While there is the possibility of low spin–high spin equilibria in nickel(II) complexes permitting binding of the second pendant alcohol in the high-spin form, the lack of any broadening or shifting of the NMR signal here appears to rule that out, and low-spin 1 : 1 complexation appears to be the rule with these ligands.

Nickel(II) in an octahedral field usually displays three absorbance bands assigned to the $^3A_{2g} \rightarrow {}^3T_{2g}$, $^3A_{2g} \rightarrow {}^3T_{1g}(F)$, and $^3A_{2g} \rightarrow {}^3T_{1g}(P)$ transitions; complexes usually display all three transitions in the visible region and are typically green to purple. In a square-planar field, the transitions change as a result of the now $e_g^4 a_{1g}^2 b_{2g}^2$ ground state configuration allowing transitions to the next empty level (b_{1g}), leading to $^1A_{1g} \rightarrow {}^1A_{2g}$, $^1A_{1g} \rightarrow {}^1B_{1g}$ and $^1A_{1g} \rightarrow {}^1E_g$ transitions with the first seen in the visible region, usually near 400 nm and the others in the near-IR region, usually above 900 nm. As a result, the complexes are usually brown. For example, the well-characterized monomeric square-planar complex of **8** has maxima at 351 nm (ε 3860), 908 nm (ε 40), and 1014 nm (ε 90); a strong band associated with π–π^* transitions of the aromatic ligand is also observed at 265 nm. In this study, the Ni(II) complex of the amino alcohol derived **3**, for example, has a band in the visible region at 361 nm (ε 1995) with an associated shoulder near 440 nm (figure 3), while no other bands are observed below 800 nm, consistent with its assignment as low-spin Ni(II). The low-energy UV band near 350 nm may actually arise from a metal–ligand charge transfer (MLCT) band involving the aromatic pyridine group, with the shoulder being the d–d band. This assignment would certainly fit with observations that square-planar low-spin Ni(II) d–d bands typically occur over a narrow range from 410 to 470 nm, depending on the nature of the donor set. A set of *o*-phenylene-dioxamidate ligands bound to Ni(II) in a square-planar manner, defined by X-ray crystallography, show a very similar behavior to this in their UV-Vis spectra [27].

The CD spectra of the nickel(II) complexes display several Cotton effects around 400 nm (figure 3, table 3), which is not consistent with the simple $^1A_{1g} \rightarrow {}^1A_{2g}$ singlet transition expected for the d–d transition but appropriate if MLCT and d–d transitions overlap in this region, as proposed above. The appearance of several Cotton effects would seem to support this proposal strongly, as there appears little other interpretation for these observations. The presence of several Cotton effects may imply that there are several species in the solution in equilibrium, possibly associated with different amounts of alcohol pendant coordination, different stereochemistries and/or possibly some high-spin species in equilibrium with the dominant low-spin form. The sensitivity of CD

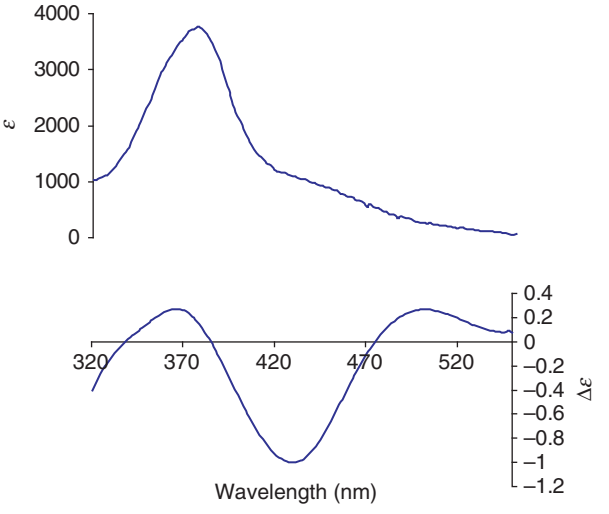

Figure 3. Visible absorbance (top) and CD (bottom) spectra of Ni^{II}(**5**-2H) in aqueous solution.

spectroscopy to such effects is well known [18]. However, these options are not really supported by any other evidence; for example, as mentioned above, no expansion of the chemical shift window or peak broadening is seen in the NMR, which might be expected if some high-spin component is present in the solution.

The d^{10} zinc(II) complex exhibits absorbance and CD spectra in the UV region, most likely to be associated with ligand-centered transitions, shifted slightly in energy as a result of deprotonation and coordination to the Lewis acid Zn^{2+}. For example, the position of the maximum for Zn^{II}(**6**-2H) and free **6** are very similar, at 273 nm and 271 nm, respectively, and the CD maxima are also very similar (260 and 285 nm for the free ligand and 255 and 292 nm for the Zn(II) complex). The observation of several CD transitions is anticipated for this ligand because of the presence of several different aromatic chromophores and nitro groups, all of which have transitions in the near UV region. Since **3** and **4**, which carry no aromatic substituents on the pendant arms, have absorption and CD maxima at or below 200 nm (table 3), the bands for **5** and **6** near 270 nm are most likely associated with the presence of a π–π^* transition of the phenyl substituents. Further, since **5** has a single Cotton effect at 245 nm and **6** has two Cotton effects at 260 and 285 nm, the second low-energy band in **6** can be assigned to the presence of the nitro group which appears only in that compound, as the higher energy band is near the position of the band in **5**, and can be assigned to the π–π^* transition of the phenyl groups. Amino acids with phenyl substituents have Cotton effects near 260 nm also [28]. The signs of the Cotton effects differ for the two bands in **6**.

4. Conclusion

The family of pyridine-diamido-dialcohol molecules prepared here, which are potential N_3O_2 donor ligands, form strong 1 : 1 complexes with transition metal ions.

Whereas the amide groups cannot be deprotonated readily in the free ligands, their deprotonation is promoted by the presence of metal ions which also bond to the deprotonated groups. As ligands, they appear superior to their parent β-amino alcohols, which are at best bidentate chelates. There is no evidence for self-assembly into oligomeric helicates, although the molecules prepared behave as efficient polydentate ligands to metal ions. In particular, because most of the examples here are chiral, there is a possibility that appropriate complexes of these molecules may find a role as catalysts for asymmetric synthesis in medicinal organic chemistry in the future, but such a study was outside the scope of this study.

References

[1] D.S. Marlin, P.K. Mascharak. *Chem. Soc. Rev.*, **29**, 69 (2000).
[2] F.A. Chavez, M.M. Olmstead, P.K. Mascharak. *Inorg. Chim. Acta*, **297**, 106 (2000).
[3] D.S. Marlin, M.M. Olmstead, P.K. Mascharak. *Inorg. Chem.*, **38**, 3258 (1999); *Inorg. Chim. Acta*, **323**, 1 (2001).
[4] Z. Xu, L.K. Thompson, D.O. Miller. *Polyhedron*, **21**, 1715 (2002).
[5] J.A. McCleverty, T.J. Meyer (Eds). *Comprehensive Coordination Chemistry II: From Biology to Nanotechnology*, Vol. 2, Elsevier Science, Oxford (2003).
[6] S.L. Jain, P. Bhattacharyya, H.L. Milton, A.M.Z. Slawin, J.A. Crayston, J.D. Woollins. *Dalton Trans.*, 862 (2004).
[7] V. Maurizot, G. Linti, I. Huc. *Chem. Commun.*, 924 (2004).
[8] N.W. Alcock, G.J. Clarkson, P.B. Glover, G.A. Lawrance, P. Moore, M. Napitupulu. *Dalton Trans.*, 518 (2005).
[9] F.A. Chavez, M.M. Olmstead, P.K. Mascharak. *Inorg. Chem.*, **35**, 1410 (1996).
[10] M. Napitupulu. Syntheses and characterisation of helical and macrocyclic complexes, PhD thesis, University of Newcastle (2005).
[11] F.A. Chavez, M.M. Olmstead, P.K. Mascharak. *Inorg. Chim. Acta*, **269**, 269 (1998).
[12] M. Napitupulu, G.A. Lawrance, G.J. Clarkson, P. Moore. *Aust. J. Chem.*, **59**, 796 (2006).
[13] W.B. Jeon, K.H. Bae, S.M. Byun. *J. Inorg. Biochem.*, **71**, 163 (1998).
[14] T.A. Neubecker, S.T. Kirksey Jr, K.L. Chellappa, D.W. Margerum. *Inorg. Chem.*, **18**, 444 (1979).
[15] G. Battistuzzi, M. Borsari, L. Menabue, M. Saladini, M. Sola. *Inorg. Chim. Acta*, **273**, 397 (1998).
[16] J.T. Stivers, C. Abeygunawardana, A.S. Mildvan, G. Hajipour, C.P. Whitman. *Biochemistry*, **35**, 814 (1996).
[17] P.M. Angus, W.G. Jackson, A.M. Sargeson. *Inorg. Chem.*, **32**, 5285 (1993).
[18] C.J. Hawkins. *Absolute Configuration of Metal Complexes*, Wiley-Interscience, New York (1971).
[19] B. Roos. *Acta Chem. Scand.*, **20**, 1673 (1966).
[20] C.J. Hawkins, C.L. Wong. *Aust. J. Chem.*, **23**, 2237 (1970).
[21] T. Yasui, J. Hidaka, Y. Shimura. *J. Am. Chem. Soc.*, **87**, 2762 (1965).
[22] C.J. Hawkins, G.A. Lawrance. *Aust. J. Chem.*, **26**, 2401 (1973).
[23] S.T.K. Bukharl, R.D. Guthrie, A.E. Scott, A.D. Wrixon. *Tetrahedron*, **26**, 3653 (1970).
[24] C.B. Barlow, R.D. Guthrie. *J. Chem. Soc. (C)*, 1194 (1967).
[25] S. Umezawa, T. Tsuchiya, K. Tatsuta. *Bull. Chem. Soc. Jpn*, **39**, 1235 (1966).
[26] R.D. Gillard, R. Wootton. *J. Chem. Soc. (B)*, 921 (1967).
[27] X. Ottenwaelder, A. Aukauloo, Y. Journaux, R. Carrasco, J. Cano, B. Cervara, I. Castro, S. Curreli, M.C. Muñoz, A.L. Roselló, B. Soto, R. Ruiz-García. *Dalton Trans.*, 2516 (2005).
[28] G. Barth, W. Voelter, H.S. Mosher, E. Bunnenberg, C. Djerassi. *J. Am. Chem. Soc.*, **92**, 875 (1970).